Developmental Cognitive Neuroscience 60 (2023) 101213

Contents lists available at ScienceDirect

Developmental Cognitive Neuroscience

journal homepage: www.elsevier.com/locate/dcn

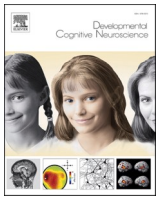

Functional maturation in visual pathways predicts attention to the eyes in infant rhesus macaques: Effects of social status

Aiden Ford [a,b,*], Zsofia A. Kovacs-Balint [d], Arick Wang [d,l], Eric Feczko [e,f], Eric Earl [g], Óscar Miranda-Domínguez [e,f], Longchuan Li [b,c,h], Martin Styner [i], Damien Fair [e,f,j,k], Warren Jones [b,c,h], Jocelyne Bachevalier [d,l], Mar M. Sánchez [d,m]

[a] Neuroscience Program, Emory University, Atlanta, GA, USA
[b] Marcus Autism Center, USA
[c] Children's Healthcare of Atlanta, GA, USA
[d] Emory Natl. Primate Res. Ctr., Emory Univ., Atlanta, GA, USA
[e] Dept. of Pediatrics, University of Minnesota, Minneapolis, MN, USA
[f] Masonic Institute of the Developing Brain, University of Minnesota, Minneapolis, MN, USA
[g] Data Science and Sharing Team, National Institute of Mental Health, NIH, DHHS, Bethesda, MD, USA
[h] Dept. of Pediatrics, Emory University, Sch. of Med., Atlanta, GA, USA
[i] Dept. of Psychiatry, Univ. of North Carolina, Chapel Hill, NC, USA
[j] Institute of Child Development, University of Minnesota, Minneapolis, MN, USA
[k] Center for Magnetic Resonance Research and Department of Radiology, University of Minnesota, Minneapolis, MN, USA
[l] Dept of Psychology, Emory University, Atlanta, GA, USA
[m] Dept. Psychiatry & Behavioral Sciences, Emory Univ., Sch. of Med., Atlanta, GA, USA

ARTICLE INFO

Keywords:
Nonhuman primate
Infant development
Social attention
Visual object pathway
Brain-behavior associations
Resting state fMRI

ABSTRACT

Differences in looking at the eyes of others are one of the earliest behavioral markers for social difficulties in neurodevelopmental disabilities, including autism. However, it is unknown how early visuo-social experiences relate to the maturation of infant brain networks that process visual social stimuli. We investigated functional connectivity (FC) within the ventral visual object pathway as a contributing neural system. Densely sampled, longitudinal eye-tracking and resting state fMRI (rs-fMRI) data were collected from infant rhesus macaques, an important model of human social development, from birth through 6 months of age. Mean trajectories were fit for both datasets and individual trajectories from subjects with both eye-tracking and rs-fMRI data were used to test for brain-behavior relationships. Exploratory findings showed infants with greater increases in FC between left V1 to V3 visual areas have an earlier increase in eye-looking before 2 months. This relationship was moderated by social status such that infants with low social status had a stronger association between left V1 to V3 connectivity and eye-looking than high status infants. Results indicated that maturation of the visual object pathway may provide an important neural substrate supporting adaptive transitions in social visual attention during infancy.

1. Introduction

In the first 6 months of life, typically developing human infants increase the amount of time they look at the eyes of others (Goren et al., 1975; Johnson et al., 1991; Valenza et al., 1996; Farroni et al., 2002; Jones and Klin, 2013). This selective social attention is a highly adaptive behavior that both initiates and maintains early social interaction, thus supporting the foundation of the infant-caregiver bond. In contrast, infants with an elevated likelihood for social disability have altered patterns of looking at faces and eyes (Jones and Klin, 2013; D'Souza et al., 2015). Though increased attention to the eyes is important for early social and cognitive development (Baron-Cohen et al., 1997; Emery, 2000), the underlying neurodevelopmental substrates associated with this basic mechanism of social attention are currently unknown. Given that early differences in attention to the eyes could serve as an indicator for atypical social development, it is imperative to understand

* Correspondence to: Marcus Autism Center, Emory University, 1920 Briarcliff Rd NE, Atlanta, GA 30329, USA.
E-mail address: aiden.l.ford@emory.edu (A. Ford).

https://doi.org/10.1016/j.dcn.2023.101213
Received 5 October 2022; Received in revised form 31 January 2023; Accepted 6 February 2023
Available online 8 February 2023

the functional development of neural systems that subserve social visual processing.

Rhesus macaques are an excellent model system for human social development because of key neuroanatomical and behavioral cross-species homologies (Machado and Bachevalier, 2003; Ghazanfar and Santos, 2004; Passingham, 2009). Their rich social environment, which is similar to that of humans, contributes to human-macaque parallels in 1) early social experiences (Ferrari et al., 2009; Dettmer et al., 2016; Powell et al., 2018; Shultz et al., 2018), 2) behavioral development (Emery, 2000; Machado and Bachevalier, 2003; Morrill et al., 2012; Wang et al., 2020), and 3) social brain organization and development (Passingham, 2009; Rilling, 2014; Kovacs-Balint et al., 2019, 2021). Both infant humans and rhesus macaques are born altricial and form strong attachments with their mothers during the first months of life. Like human infants, infant rhesus macaques show preferences for face-like stimuli and direct gaze from birth (Kuwahata et al., 2004; Parr, 2011; Muschinski et al., 2016; Parr et al., 2016). Importantly, Wang et al., 2020 showed that developmental trajectories of looking at the eyes of conspecifics in infant macaques and human infants are highly homologous.

The early social experiences of infant rhesus monkeys are fundamentally shaped by their social status, which is determined by their mother's family rank in their group's social dominance hierarchy (White and Hinde, 1975; de Waal and Luttrell, 1985; Snyder-Mackler et al., 2016; Wooddell et al., 2020). Low-ranking, or subordinate, animals face a harshly disparate social landscape. They are subject to continuous aggression and harassment from more dominant animals (Berman, 1980; de Waal and Luttrell, 1985), show higher vigilance/anxiety, and receive less affiliative behaviors from other animals in the group (Bernstein et al., 1974; Bernstein, 1976, 1988; Godfrey et al., 2016). Therefore, low social status (LSS) constitutes a chronic psychosocial stressor, similar to socio-economic adversity in humans (Wilson, 2016). Rank also influences their patterns of visual attention as infant macaques learn to visually navigate their social environment. In the first month of life, LSS infants look less to the eyes of conspecifics than high social status (HSS) infants (Paukner et al., 2018) and by 9 months of age, look less at threatening faces (Mandalaywala et al., 2014). Social signals defining the social status hierarchy are conveyed through gaze and facial expression (Mosher et al., 2011), so decreased social attention in LSS infants may indicate they have learned to avoid staring at aggressors, which is a threatening expression that may represent a challenge. However, how social rank influences longitudinal change in social visual attention and its underlying neurobiology remains unknown.

Modeling human social development in rhesus macaques has important practical advantages. Rhesus macaques have an accelerated developmental trajectory that allows for longitudinal data collection in a quarter of the time needed to collect data from human infants (e.g. if one wants to model the first 2 years of human life, data collection in macaques would take place over 6 months (Mattison and Vaughan, 2017)). With macaque infants, we can also control for relevant confounding variables, e.g., nutrition, resource access, maternal care, and prenatal exposure to drugs, and collect data at a higher sampling density and image resolution, which particularly benefits neuroimaging studies.

Longitudinal neuroimaging studies with human infants and infant macaques show critical similarities in brain development between species. In both species, the first months of life mark the most rapid period of postnatal structural growth, with occipital cortex in particular showing concentrated expansion (Li et al., 2013b; Gilmore et al., 2018; Kovacs-Balint et al., 2021). Combined with findings from functional studies showing that primary sensory networks and structures mature before integration and association networks (Deoni et al., 2011; Gao et al., 2015; Kovacs-Balint et al., 2019, 2021), there is substantial evidence of a caudal to rostral progression of brain maturation in both human infants and infant macaques.

To investigate possible neural mechanisms associated with change in social visual attention in the first months of life, we focused on the development of functional connectivity (FC) between regions in the ventral visual pathway, also called the visual object pathway. Comprised of the primary visual area (V1), extrastriate visual area (V3), inferior temporal areas (TEO, TEp), and the amygdala (AMY), the visual object pathway facilitates social cognition in adult rhesus macaques and humans (Pitcher and Ungerleider, 2020; Kosakowski et al., 2021). This role stems from connections to key regions involved in the processing of gaze cues and facial expressions – the superior temporal sulcus (STS) and the face patch, which is an inferior temporal cortex region analogous to the fusiform gyrus, "Fusiform Face Area", in humans (Ku et al., 2011; Ungerleider and Bell, 2011). Inactivation of the left posterior STS suppresses gaze following behavior in adult rhesus macaques (Roy et al., 2014). Developmentally, evidence indicates these regions are sensitive to social information from birth (Rodman et al., 1991; Arcaro and Livingstone, 2017) and then refine through experience-dependent processes (Webster et al., 1991a; b). In infant macaques, the face patch emerges gradually over the first 5 to 6 months (Livingstone et al., 2017) and this developmental window appears to be a critical period as infant macaques who grow up without exposure to conspecific faces do not have face patch regions in adulthood (Arcaro et al., 2017). A previous study from our group charted the maturation of the visual object pathway from 0 to 3 months and found that FC along this pathway undergoes substantial remodeling during this period of intense social exposure. That remodeling contrasted with change measured in the motion and visuo-spatial pathways in which FC between cortical areas was still weak during the first 3 months of life (Kovacs-Balint et al., 2019). Therefore, the visual object pathway is a compelling target for an investigation into the neural pathways associated with social visual attention.

In summary, this study aimed to map developmental trajectories of FC along the visual object pathway and attention to the eyes of conspecifics from 0 to 6 months using non-parametric longitudinal modeling. We then assessed how social rank influences the timing of attentional milestones in eye-looking. Finally, in an exploratory analysis, we tested for associations between developmental features of trajectories of brain and behavior to examine whether development of the visual object pathway predicts social attention to the eyes.

2. Materials and methods

2.1. Subjects and housing

Male infant rhesus monkeys (*M. mulatta*), total N = 38, completed longitudinal eye-tracking and resting state functional connectivity (FC) data collection during their first 6 months of life. These protocols were part of a broader programmatic study that also investigated trajectories of structural brain development (Kovacs-Balint et al., 2021). This study included only male infants given the increased prevalence of neurodevelopmental disability associated with social-cognitive difficulties in human males: autism, ADHD, schizophrenia, and communication delays (Santos et al., 2022). Moreover, increasing evidence implicates exposure to pre- and/or postnatal psychosocial stressors as a contributing factor in atypical neurodevelopmental outcomes (May et al., 2019).

A subset of these infants, N = 31, had usable eye-tracking data and another subset, N = 21, had quality scans for resting-state functional analyses (for quality assessment steps see *2.3 Resting-state functional Magnetic Resonance Imaging (rs-fMRI)* and *2.4 Eye-tracking procedures)*. Between these two cohorts, 14 infants had data of both modalities (Fig. 1). Infants were excluded from the study per the following criteria: 1) low birth weight (<450 g), 2) born to a primiparous mother, 3) born to a mother with a history of, or current, poor maternal care, and 4) significant medical or behavioral issues. All subjects lived in complex social groups with their mothers and families at the Emory National Primate Research Center (ENPRC) Field Station, in Lawrenceville, GA (RRID: SCR_001914). This environment provided the species-typical social experience fundamental to infants' development. Social groups

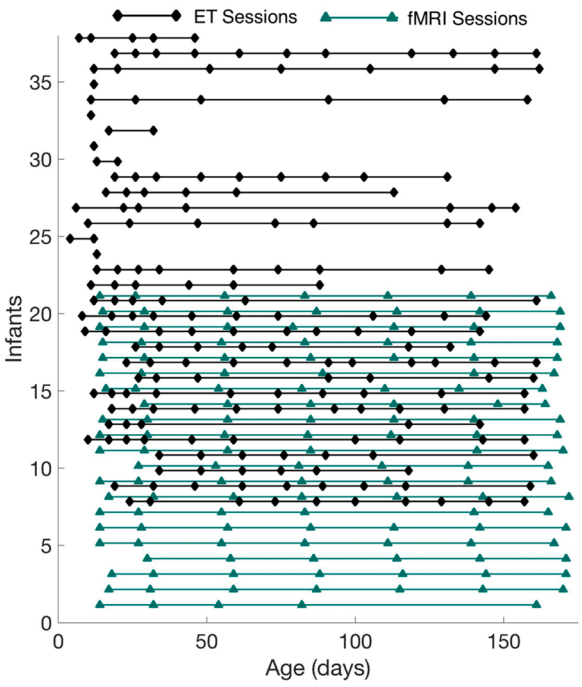

Fig. 1. Distribution of fMRI scans and eye-tracking sessions for infant rhesus macaques. Twenty-one infants had fMRI scans (average 6.7 per infant), and 31 infants had eye-tracking sessions (average 6.5 per infant), with 14 animals having data from both modalities. Full details of included scan and eye-tracking data are provided in Supplementary Materials. ET – eye-tracking; fMRI – functional magnetic resonance imaging.

had 55 to 130 adult females with their offspring, and 2 to 4 adult males, and were housed in large compounds with outdoor and climate-controlled indoor areas. Animals were fed standard monkey chow (Purina Mills Int., Lab Diets, St. Louis, MO) and water was freely available. Animals also had fruits and vegetables twice daily, and additional enrichment. All study protocols were approved by the Emory University Institutional Animal Care and Use Committee (IACUC) in accordance with the Animal Welfare Act and the U.S. Department of Health and Human Services "Guide for Care and Use of Laboratory Animals."

2.2. Social status

Infant social status/rank was determined directly before birth by the Colony Management team at the ENPRC and reflects their matrilineal social rank, i.e., the status of their family relative to the rest of families within their respective social hierarchy. Infants and their families were monitored throughout the 6-month duration of this study and ranks remained stable.

Rank was measured through behavioral observations of individual, family, and group dynamics following established methods (Bernstein, 1976; Embree et al., 2013; Howell et al., 2014; Pincus et al., 2021). Two behaviors were used to define social subordination: rates of aggression received and submissive behavior emitted by the subject (Bernstein, 1976). Ranks were normalized to a percentile, with low percentiles representing relatively lower infant social rank. For example, an infant with rank 3 out of 10 indicates they were born into the third-top ranked family out of 10 families total. Their percentile would be 70%. Rank information (relative, percentile) from the subjects with both eye-tracking and rs-fMRI data is shown in Table 1.

2.3. Resting-state functional Magnetic Resonance Imaging (rs-fMRI)

Details of this protocol were previously published in Kovacs-Balint et al. (2019). Below we provide a summary of key methodological steps.

Table 1
Social rank for infant subjects with both eye-tracking and rs-fMRI data. Percentile reflects the lower bound of subject rank and subjects were organized from highest to lowest rank. Subject 4 rank was adjusted from 0% to 1%.

Animal Number	*Social Rank (Relative)*	*Social Rank (Percentile)*
10	2 of 10	80%
1	3 of 13	76.9%
7	3 of 11	72.7%
13	2 of 5	60%
12	6 of 13	53.8%
3	3 of 5	40%
9	3 of 5	40%
6	7 of 11	36.4%
11	9 of 13	30.8%
2	7 of 10	30%
5	4 of 5	20%
14	10 of 11	9.1%
8	12 of 13	7.7%
4	10 of 10	1%

2.3.1. MRI image acquisition

Structural and resting-state functional MRI data were collected from infant macaques at up to 7 times through the first 6 months of life, at 0.5, 1, 2, 3, 4, 5, and 6 months of age (approximately 14, 28, 56, 84, 112, 140, and 168 days old). Of note, we expanded the dataset analyzed in Kovacs-Balint et al. (2019) by adding 11 animals and 3 later scanning timepoints at 4, 5, and 6. On the day of each scan, infants were transported to the ENPRC Imaging Center with their mothers. They then returned the next day for veterinary monitoring. All infants were scanned using an 8-channel phase array head coil on a 3 T Siemens Magnetom Trio Tim scanner. To minimize motion artifacts, infants were intubated and anesthetized using telazol (2.34 ± 0.55 mg/kg body weight) and isoflurane (0.8–1% via inhalation), as low as possible to limit the effect of anesthesia on the blood-oxygen-level-dependent signal (BOLD) used to index brain activity (Vincent et al., 2007; Hutchison et al., 2013; Li et al., 2013a; Miranda-Dominguez et al., 2014). During each imaging session, we collected a high-resolution T1- and T2-weighted structural scan (T1 parameters: 3D magnetization prepared rapid gradient echo (3D-MPRAGE) parallel image sequence, inversion time = 900 ms, TR/TE = 2600/3.46 ms, voxel size: 0.5 mm^3 isotropic; T2 parameters: TR/TE = 3200/373 ms, voxel size: 0.5 mm^3 isotropic) and two 15-minute rs-fMRI BOLD images using a T2 * -weighted gradient-echo echoplanar imaging (EPI) sequences (EPI parameters: 400 volumes, TR/TE = 2060/25 ms, voxel size: 1.5 mm^3 isotropic), with a reverse phase encoding rs-fMRI scan collected for distortion correction in the EPI scans (Andersson et al., 2003).

2.3.2. Rs-fMRI data processing

All processing steps were completed using the FMRIB Software Library (FSL, Oxford, UK, RRID: SCR_002 823; (Smith et al., 2004; Woolrich et al., 2009)), 4dfp tools, and a Nipype-based pipeline built in-house (Gorgolewski et al., 2011). To improve signal-to-noise ratio and reduce signal artifacts, functional images underwent 1) unwarping using TOP-UP correction (Andersson et al., 2003), 2) slice-time correction, 3) motion correction, and 4) signal normalization. Motion correction included 1) within-run rigid body correction, 2) linear registration of EPI to T1, and 3) nonlinear registration of T1 to template.

Subjects' EPI functional images were registered to their own T1-weighted structural images, which, in turn, were nonlinearly registered to age-specific rhesus macaque structural MRI atlases developed by our group (Shi et al., 2016) (available at https://www.nitrc.org/projects/macaque_atlas). Based on best match of neuroanatomical characteristics, infant scans completed at 0.5 and 1 months were registered to the 0.5-month atlas, scans completed at ages 2, 3, and 4 months were registered to the 3-month atlas, and scans at 5 and 6 months were

registered to the 6-month atlas. Additional steps consisted of 1) detrending the functional signal, 2) removal of nuisance regressors using global signal regression, and 3) application of a second-order Butterworth filter (Fair et al., 2007, 2009, 2012; Miranda-Dominguez et al., 2014). Use of global signal regression is explained and justified in further detail in Kovacs-Balint et al. (2019).

2.3.3. Functional connectivity analysis

FC values were generated between 5 regions-of-interest (ROIs) along the visual object pathway: visual areas V1-V3, inferior temporal regions, TEO and TEp, and the amygdala, AMY (see Fig. 2 for schematic of the full pathway). These ROIs were defined using 3 parcellation schemes. Label maps for the left and right AMY were manually delineated (Styner et al., 2007) and propagated to the UNC-Emory rhesus infant atlases via ANTS (Shi et al., 2016). Remaining ROIs were mapped from established parcellations (Lewis and Van Essen, 2000; Markov et al., 2014) to the UNC-Emory atlas space. All ROIs were then evaluated and, if necessary, manually edited by experimenters in a quality control step to ensure neuroanatomical accuracy and prevent ROI overlap and signal drop out.

For each subjects' scans, FC values were calculated for every ROI in the visual object pathway. BOLD timeseries across all the voxels within each distinct ROI were averaged to determine the overall ROI FC value. These values were then correlated with the FC values of the other ROIs along the visual object pathway, creating a pathway-specific correlation matrix. The resulting R-coefficients were then transformed into Fisher Z-scores, which were used to build longitudinal trajectories of change in FC. A Z-score of 0 corresponds to undetected FC between two regions, meaning the two regions are not temporally correlated, i.e., functionally coupled.

2.4. Eye-tracking procedures

The complete behavioral protocol has been published in Wang et al. (2020). Below is a condensed summary.

2.4.1. Procedure

Eye-tracking data was collected up to 14 times in the first 6 months (at approximately 7, 14, 21, 28, 35, 49, 63, 77, 91, 105, 119, 133, 147, and 161 days old). Mother-infant dyads were transferred to the onsite behavioral testing facility at the ENPRC Field Station. Before eye-tracking began, mothers were lightly anesthetized and placed comfortably on a seat in the testing room. The infant was settled onto her ventrum, so it could easily view the monitor screen attached to the wall. An infrared camera captured the infant's eye image and was controlled by an experimenter to dynamically calibrate and track the eye image during testing.

2.4.2. Stimuli

Infants watched high quality digital videos of novel conspecifics filmed at the Caribbean Primate Research Center breeding colony in Cayo Santiago, Puerto Rico (for details see Wang et al., 2020). At the start of each session, the infant's gaze was calibrated to the eye-tracking software using a 5-point calibration procedure (Jones and Klin, 2013). Once the calibration was validated, infants watched randomized video playlists until 30 minutes had passed. A centering stimulus played between each video to confirm calibration accuracy, or to repeat the calibration procedure. If infants had a clear eye-image, a consistently accurate calibration, and fixated on the screen for $\geq$ 20% of a given video's duration, data were then screened and selected for analysis. For age-specific details of calibration success and total videos watched, please see Wang et al., 2020.

2.4.3. Data analysis

In-house software implemented in MATLAB was used to parse all recorded data into distinct categories of eye movements: fixations, blinks, saccades, and missing data (offscreen fixations or otherwise missing time series data due to head movements or other artifacts) (Jones and Klin, 2013). Video content was parsed into predetermined Regions of Interest (ROIs), each containing specific categories of visual

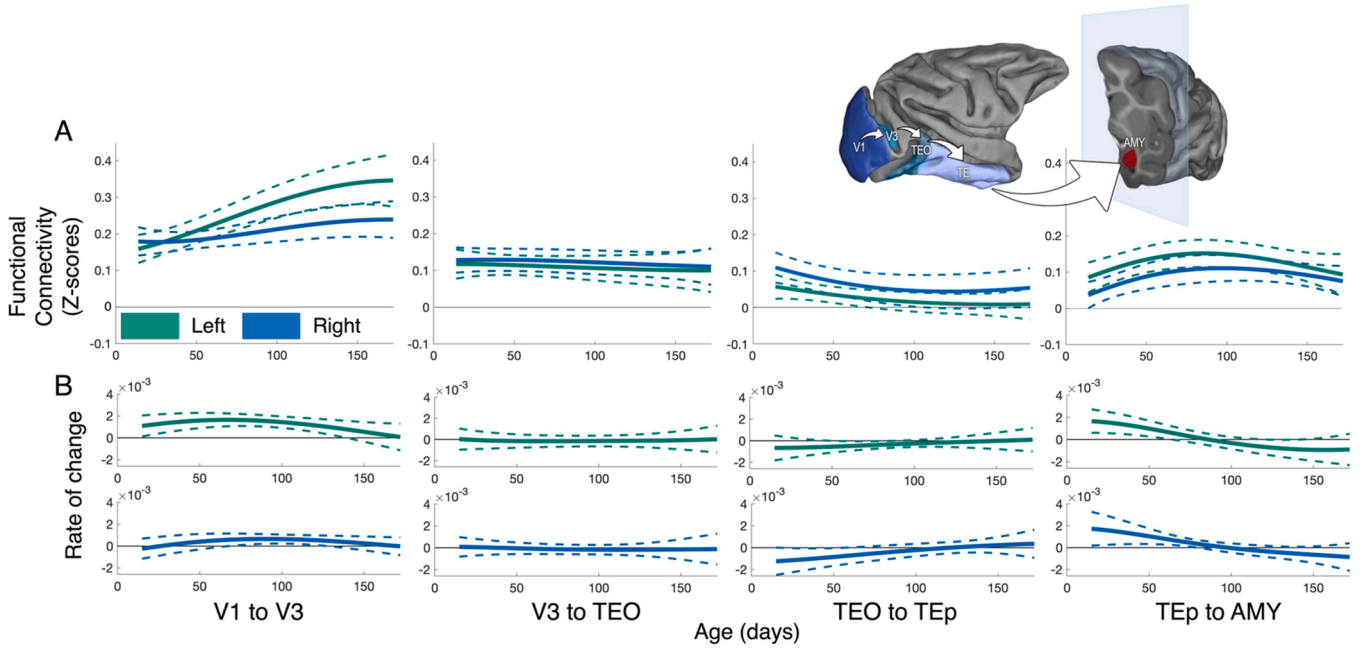

Fig. 2. Functional connectivity from 0 to 6 months in the visual object pathway shows maturation patterns unique to each region-region pair. Thick line denotes rate of change trajectory and thin dashed lines denote 95% simultaneous confidence bands. A) Trajectories of connectivity between V1 to V3, V3 to TEO, TEO to TEp, and TEp to AMY in the left and right hemispheres from 0 to 172 days (0 to 6 months). Z-scores of 0 correspond to undetected FC between two regions, meaning signal between the two is not temporally correlated. B) Trajectories of rate of change for group mean trajectories from A. Rate of change for trajectories in the left and right hemispheres in the first and second rows, respectively. Periods of significant change occur when the confidence bands are above or below the zero line. V1 - primary visual area; V3 - extrastriate visual area; TEO and TEp - inferior temporal areas; AMY - amygdala. Regions visualized in the connectivity schematic (upper left), adapted from Kovacs-Balint et al. (2019) with permission.

information: eyes, mouth, and body of the conspecific in the video, and the scene background. Analyses were conducted at the video frame rate of presentation, 30 Hz. The percent of total viewing time spent fixating on these regions was calculated for each video watched by the subject and used to model longitudinal growth curves. In this analysis, we mapped the trajectory for attention to the eyes.

2.5. Statistical analyses

2.5.1. Longitudinal data analysis

Previous analyses used traditional polynomial models and analyses of variance to show evidence of non-linear developmental change in trajectories of FC in the visual object pathway and in trajectories of eye-fixation (Kovacs-Balint et al., 2019; Wang et al., 2020). These findings motivated further study of these trajectories, specifically the identification of key inflection points and potential brain-behavior relationships during infancy. To achieve this aim, we implemented a non-parametric curve-fitting approach specifically designed for sparse longitudinal data. Functional Principal Components Analysis (FPCA) incorporates functional data analysis and empirical dynamics methods to offer unique advantages for modeling sparse longitudinal data (Yao et al., 2005; Chen et al., 2021). First, FPCA is designed to handle datasets with non-uniform sampling and missing data points, a common reality in longitudinal developmental data. Second, FPCA places no assumptions on the underlying shape of the growth curve, relying on a data-driven algorithm to extract curve shape. Third, alongside the group mean, FPCA constructs individual trajectories, allowing for between-subject comparisons of developmental change.

Group mean and individual growth curves of developmental change were built for both the eye-tracking and FC datasets using FPCA in MATLAB, version R2019b (Yao et al., 2005). Mean curves were fit using a gaussian kernel and rates of change were determined by calculating the first derivative of the mean curve. The shape of the group mean and rate of change curves were confirmed with 95% confidence using bootstrapped simultaneous confidence intervals. In the bootstrapping procedure, data was resampled with replacement at the individual level over 1000 iterations. For each iteration of resampled data, a new group mean curve and rate of change curve were calculated. The group mean curves from all iterations were used to derive the simultaneous confidence intervals for the original mean curve and the rate of change curves from all iterations were used to derive the simultaneous confidence intervals for the original rate of change curve.

One-tailed t-tests and Cohen's d calculations were used to verify inter-hemispheric differences in FC between region-region pairs. These tests were performed on the data from each scanning time point – 0.5, 1, 2, 3, 4, 5, and 6 months.

Patterns of variance in individual data relative to the mean curve were extracted by FPCA and represented as principal component (PC) functions. PC functions from FPCA are like the components extracted in standard Principal Components Analysis, except they capture patterns of variance that unfold over time. Each PC function is orthogonal to the others and explains a certain percentage of total variance over the entire trajectory. For these reasons, PC functions can provide information about important developmental features of trajectories, including the magnitude and timing of inflection points (Jones and Klin, 2013; Dai et al., 2019b, 2019a). Trajectories for individual subjects can be decomposed into a weighted mixture of extracted PC functions. As a result, individuals are assigned values that quantify the extent to which their own trajectory follows the variance pattern of each PC function – these values are called PC scores. For example, if 2 PC functions are extracted for a group mean trajectory (PC1 and PC2), individuals in the sample will each have 2 separate PC scores (PC1 score and PC2 score), with each score signifying the shape of their trajectory relative to the shape of a PC function. PC scores are scalar values and thus can be modeled into parametric univariate and multivariate analyses (Wang et al., 2015).

2.5.2. Statistical models

In the subsample of 14 animals with both eye-tracking and neuroimaging data, bi-variate and multiple linear regression models were used in an exploratory analysis of relationships between FC development in the visual object pathway, attention to the eyes of others, and infant's social rank. Analyses were completed in MATLAB version R2019b and SPSS Statistics 27. Multiple regression models included 3 predictive factors: PC scores from trajectories of brain development, infant social rank, and an interaction term. PC scores from trajectories of eye-looking were modeled as the response variable.

3. Results

3.1. Functional connectivity in the visual object pathway

To optimize FPCA curve-fitting performance (Yao et al., 2005), data from all infant macaques with quality fMRI sessions (N = 21) were included to build trajectories of functional connectivity (FC) development between ROIs in the visual object pathway in the right and left hemispheres, as well as the rates of change (Fig. 2).

FC between V1 and V3 increased from 0 to 6 months and was significantly leftward lateralized by day 110, about 4 months. FC values in the left hemisphere more than doubled from 0 to 6 months, increasing from 0.16 to 0.35, whereas in the right hemisphere, FC values increased from 0.18 to 0.24. Significant differences between mean FC on the left and right were confirmed at 3 ($t(20) = 3.5$, Cohen's d 0.76), 4 ($t(18) = 4.1$, Cohen's d 0.97), 5 ($t(19) = 3.8$, Cohen's d 0.85) and 6 months ($t(20) = 3.3$, Cohen's d 0.72) using paired one-tailed t-tests with post-hoc Bonferroni correction ($p < .005$). Strengthening FC was driven by significantly positive rates of change in both hemispheres, though the period of significant change lasted longer in the left hemisphere, from 0 to 139 days (0 to 5 months) versus 67 to 128 days (2.4 to 4.5 months) on the right. FC between V3 and TEO was consistently positive and showed a slight decrease in the first 6 months, though there were no periods marked by significant rates of change. FC between TEO and TEp decreased in both hemispheres, with significant periods from 49 to 90 days (1.8 to 3.2 months) on the left and 0 to 57 days (0 to 2 months) on the right. In later infancy, the confidence intervals for the trajectory of FC in left TEO to TEp cross 0, indicating no significant coupling between the two regions (Fig. 2A). Finally, FC between TEp and AMY increased until 3 months (86 and 97 days in the left and right hemisphere, respectively), and then decreased, ultimately to values comparable to those measured at 0.5 months. FC between TEp and AMY was significantly leftward lateralized at 0.5 months ($t(17) = 2.5$, Cohen's d 0.59), but this result did not survive post-hoc Bonferroni correction ($p < .005$).

FC between each pair of regions in the visual object pathway showed a distinct developmental shape. Baseline FC was highest between V1 and V3 and lower in region-region pairs in inferior temporal areas and AMY. FC remained strongest between V1 and V3 throughout the first 6 months of life. The rate of change across the growth curves revealed the first 3 months to be a particularly dynamic period with V1 to V3, TEO to TEp, and TEp to AMY all registering periods of statistically significant strengthening or weakening FC. The 0 to 3 month change patterns quantified in this sample were highly consistent with those measured using standard analyses of variance in a subset of this sample (N = 10) in Kovacs-Balint et al. (2019).

3.2. Developmental change in attention to the eyes

Again, to optimize FPCA curve-fitting performance, data from all infants with quality eye-tracking sessions (N = 31) were included to build the trajectory of attention to the eyes (Fig. 3). Percent fixation to the eyes increased through the first 2 months of life and then plateaued. This pattern may represent a visual attention milestone for infant macaques, parallel to the increased social exploration and mobility that takes place around this age (Suomi, 2005). The rate of change in

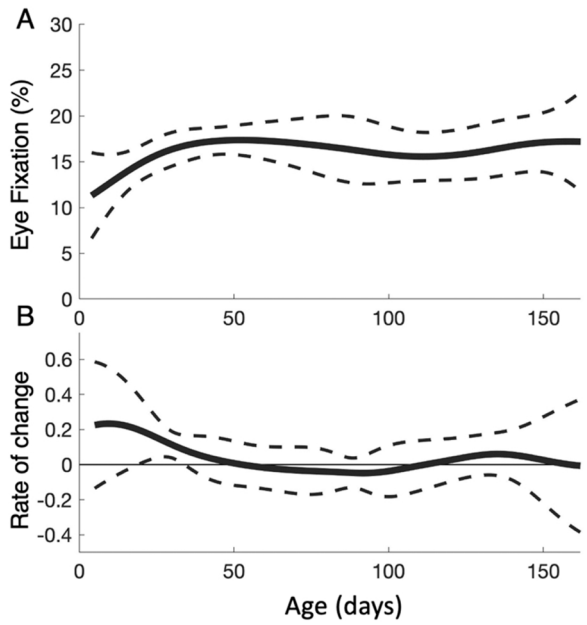

Fig. 3. Trajectory of attention to the eyes of conspecifics from 0 to 6 months. Thick line denotes rate of change trajectory and thin dashed lines denote 95% simultaneous confidence bands. A) Trajectory of percent fixation to the eyes from 0 to 162 days (0 to 6 months). B) Trajectory of rate of change (% per day) for group mean trajectory from A. Periods of significant change occur when the confidence bands are above or below the zero line.

eye-looking was significantly positive from 19 to 34 days (0.7 to 1.3 months). Wider confidence intervals indicated two periods of increased variability about the group mean, 70 to 100 days (2.5 to 3.5 months), and 140 to 162 days (5 to 6 months). Visualization of individual trajectories verified these periods as highly variable across individuals (Fig. 4).

This eye-tracking trajectory, mapped using FPCA, was consistent with a prior analysis of this data that used a traditional polynomial model, published in Wang et al. (2020). However, these results did not show the same reported mean increase at 6 months (~160 days) as Wang et al. (2020). Our results instead indicated increased individual variability at that age.

3.3. Effect of social status on trajectories of attention to eyes

Previous cross-sectional studies in rhesus macaques showed that social rank moderates attention to the faces of others during infancy (Mandalaywala et al., 2014; Paukner et al., 2018). Considering that social attention changes rapidly over the first 6 months of life, we investigated the effect of social status on attention to the eyes using a longitudinal approach.

The group mean trajectory of attention to the eyes had two major developmental patterns that varied between individuals. Those two variance patterns, quantified by FPCA in principal component functions (PC1 and PC2), each span the entire 0 to 6-month period of interest, but are most pronounced during specific developmental windows (Fig. 4A). Two PC scores, one for each component, were computed for every subject. These scores quantified the extent to which their individual trajectory followed the variance pattern of PC1 or PC2. PC1 quantified individual variability in eye-looking during later infancy, with positive scores indicating larger increases in later eye-looking and negative scores indicating decreases in later eye-looking (Fig. 4A). PC2 quantified individual variability in the timing of the increase in eye-looking from 0 to 100 days, with positive scores indicating an earlier plateau in eye-looking and negative scores indicating a later plateau (Fig. 4A). PC 1 explained 91.6% of variance in individual data relative to the mean trajectory and PC 2 explained 8.4% of variance.

Bi-variate regressions between social rank and individual PC scores from PC1 and PC2 were used to examine the effects of social status on individual trajectories of attention to the eyes. These models showed trending relationships ($p = .09$, $p = 0.055$) in the subsample of 14 animals with dual data. Each PC function highlighted variability in eye-looking during specific developmental windows, so more targeted measures of that variability were derived to increase signal. We tested for relationships between social rank and the targeted measure from each PC: from PC1, the rate of change from 3.5 to 6 months (range −0.054 to 0.13% change per day) and from PC2, the age at which the increase in eye-looking plateaus (range 37 to 60 days) (Fig. 4A). Infant rank was significantly associated with both the slope of an individual's eye-looking trajectory in later infancy ($R^2 = 0.30$, $p < .05$) and the age of the plateau in eye-looking in early infancy ($R^2 = 0.39$, $p < .05$). LSS infants exhibited accelerated trajectories of eye-looking, reaching their initial peak in eye-looking earlier than their HSS peers, and on average, looking more to the eyes of others in later infancy (Fig. 4B).

3.4. Exploratory brain-behavior associations

To test whether FC along the visual object pathway predicted either or both major developmental patterns in infant eye-looking behavior, represented by eye-looking PC1 and PC2 (Fig. 4A), we focused on region-region pairs where FC trajectories showed significant rates of change: between left and right V1 to V3, TEO to TEp, and TEp to AMY. For each of these FC trajectories, the first principal component (PC1) reflected variance related to the magnitude of individual FC trajectories, such that individuals with more positive FC PC1 scores would have a greater overall increase and/or decrease in FC in that region-region pair relative to the group mean and vice versa for individuals with negative scores (see Fig. 5A,C for visualization of PC1 functions for FC in left and right V1 to V3, see Fig. S2 for visualization of all PC functions for each region-region pair in visual object pathway). Multiple regression models were built to determine if individual eye-looking PC1 or PC2 scores could be predicted from each region-region pairs' FC PC1 scores, infant social rank, and an interaction term (PC1 scores*social rank) (see Tables S3 and S4 for outputs from these models). This approach allowed us to test whether longitudinal change in FC along regions in the visual object pathway was associated with longitudinal change in eye-looking and how social rank potentially impacted that brain-behavior relationship.

Increases in FC between left V1 to V3 (measured through FC PC1 scores) significantly predicted an earlier increase and plateau in eye-looking (measured by eye-looking PC2 scores) (model uncorrected $p = 0.018$) (Fig. 5). There was also a significant interaction between increasing FC in left V1 to V3 and social rank, such that for LSS infants, every increase in their left V1 to V3 FC PC1 score resulted in a 4.08 unit increase in their eye-looking PC2 score (derived from the estimated beta values in Fig. 5D). Referencing Fig. 5, for LSS infants, greater overall increases in FC between left V1 and V3 – such that their individual trajectory of FC in left V1 to V3 reflects the shape represented by the (+) symbols in Fig. 5A – predict that they will reach their initial plateau in eye-looking earlier – such that their individual eye-looking trajectory reflects the shape represented by the (+) symbols in Fig. 5B. This relationship was different for HSS infants: each increase in their FC PC1 score resulted in a 1.27 unit *decrease* in their eye-looking PC2 score (derived from the estimated beta values in Fig. 5D). Again referencing Fig. 5, for HSS infants, greater overall increases in FC between left V1 and V3 – such that their individual trajectory of FC in left V1 to V3 reflects the shape represented by the (+) symbols in Fig. 5 A – predict that they will reach their initial plateau in eye-looking *later* – such that their individual eye-looking trajectory more closely follows the shape represented by the (-) symbols in Fig. 5B. To summarize, these results indicate a differential brain-behavior relationship relative to infant social status. For LSS infants, increasing FC in left V1 to V3 predicted more

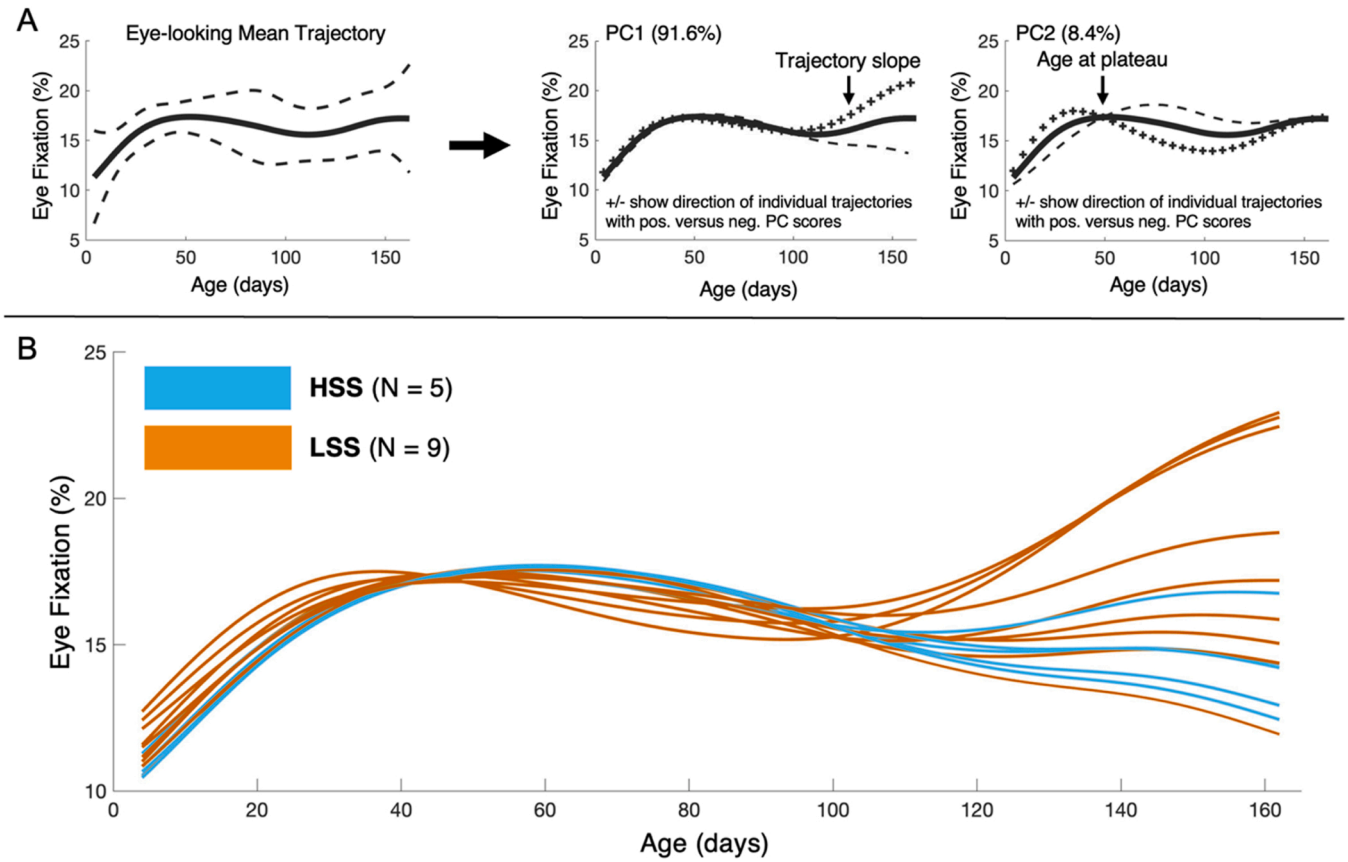

Fig. 4. Social status moderates shape of eye-looking trajectories for individual infants. A) Patterns of variance in individual trajectories relative to the mean growth curve are quantified in principal component (PC) functions. PCs are plotted around the group mean trajectory (solid line). Major features of each component – from PC1, trajectory slope from 3.5 to 6 months and from PC2, age at trajectory plateau – were associated with infant social status. B) Individual eye-looking trajectories from 14 infants with both ET and rs-fMRI data are categorized by social rank. Lower ranked infants have an earlier plateau in eye-looking ($p < .05$) and greater increases in eye-looking from 3.5 to 6 months ($p < .05$). Abbreviations: HSS (high social status) – infant is born into top 50% of ranked families, LSS (low social status) – infant is born into bottom 50% of ranked families. Pos. – positive, neg. – negative.

accelerated trajectories of eye-looking than for HSS infants. Social rank did not independently predict whether infants had an overall greater or lesser increase in left V1 to V3 FC ($p > .05$). Importantly, this brain-behavior relationship was specific to eye-looking. FC between left V1 and V3 did not predict developmental changes in attention to the mouth or body (Figs. S3 and S4).

PC1 scores from right V1 to V3 showed a trend towards predicting eye-looking PC2 scores (model uncorrected $p = .51$), motivating future study of this region in larger samples. PC1 scores from no other regions along the visual object pathway predicted eye-looking PC2 scores and PC1 scores from no visual object regions predicted eye-looking PC1 scores (Tables S3 and S4). The brain-behavior results did not survive false discovery correction, which was expected considering the exploratory nature of this analysis and our comparatively small sample size ($N = 14$). Moreover, we modeled relationships between variables that capture long-scale features of developmental change during a highly dynamic period of neurobehavioral growth. Therefore, we look forward to continued study in this area and encourage the use of longitudinal study designs and non-parametric modeling approaches to replicate and extend these results.

4. Conclusions

In this paper, we mapped the developmental trajectories of looking to the eyes of conspecifics and functional connectivity (FC) between brain regions that process socio-visual information along the visual object pathway from birth to 6 months in infant rhesus macaques. During this period, significant change in FC was measured within the primary visual regions (V1-V3), inferior temporal regions (TEO-TEp), and between the inferior temporal regions and the amygdala (TEp-AMY). There was no change in FC between the extrastriate areas and the inferior temporal region (V3-TEO). Social visual attention patterns also revealed a period of dynamic change, with eye-looking increasing from birth to 2 months and then plateauing.

Using nonparametric longitudinal modeling, we also present evidence that stronger increases in FC between the left primary and extrastriate visual areas (V1-V3) predict earlier increases in visual attention to the eyes of conspecifics in the first 2 months of life. This association was moderated by infant social status, such that LSS infants showed an accelerated maturation of eye-looking patterns and reach a key transition in social visual attention earlier in development. This difference could be a neurobehavioral adaptation to prepare subordinate infants to process salient socio-visual cues earlier in life and better navigate their complex social environment. Together, these results cement the first months of life as a significant period of neurobehavioral maturation and indicate visual cortex maturation supports social visual attention in the earliest weeks of life.

4.1. Connectivity along the visual object pathway

From birth to 6 months, FC along the visual object pathway changes rapidly, charting distinct region-to-region trajectories and developmental shapes (Fig. 2A). The trajectories presented here replicate and extend the 0 to 3 months trajectories analyzed in a subsample of these

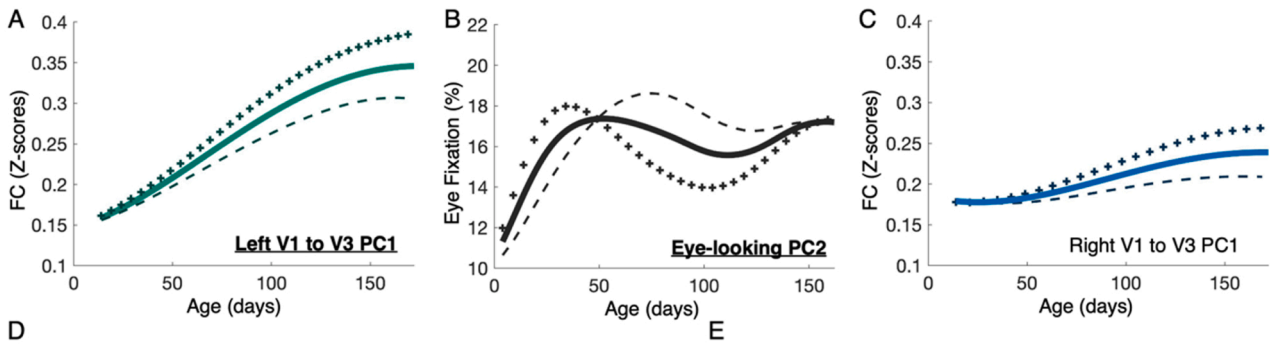

D

Prediction of Eye-looking PC2 Scores from Left V1 to V3 PC1 Scores & Social Rank: *Model adjusted R^2 = 0.51, uncorrected p = 0.018*

	Estimated Beta	*t*	*p*
Intercept	1.58	1.62	0.14
Left V1toV3 PC1 Scores	4.08	3.26	0.009*
Social Rank	-2.42	-1.17	0.27
*Left V1toV3 PC1 Scores*Social Rank*	-5.35	-2.51	0.03*

E

Prediction of Eye-looking PC2 Scores from Right V1 to V3 PC1 Scores & Social Rank: *Model adjusted R^2 = 0.38, uncorrected p = 0.051*

	Estimated Beta	*t*	*p*
Intercept	2.45	2.34	0.04
Right V1toV3 PC1 Scores	-4.31	-2.52	0.03
Social Rank	-3.91	-1.67	0.13
*Right V1toV3 PC1 Scores*Social Rank*	6.97	1.72	0.12

Fig. 5. Magnitude increases in functional connectivity (FC) of left V1 to V3 differentially predict developmental patterns in eye-looking for LSS versus HSS infants (p = 0.018). A-C) Extracted principal components (PCs) of variance are plotted around the group mean trajectory (solid line). + /- indicate the direction of individual trajectories with positive versus negative PC scores. Bolded labels highlight components with correlated scores. A) PC1 of the trajectory of left hemisphere V1 to V3 FC. B) PC2 of the eye-looking trajectory. C) PC1 of the trajectory of right hemisphere V1 to V3 FC. D) Output statistics of the multiple regression model including PC1 scores from left V1 to V3 FC, social rank, and an interaction term as the predictive factors, and PC2 scores from eye-looking trajectory as the response. E) Output statistics of the multiple regression model including PC1 scores from right V1 to V3 FC, social rank, and an interaction term as the predictive factors, and PC2 scores from eye-looking trajectory as the response. *marks factors from significant models with p-value less than an alpha value of 0.05. V1 – primary visual area; V3 – extrastriate visual area.

infants by Kovacs-Balint et al. (2019). The rate of change across the growth curves revealed the first 3 months to be a particularly dynamic period with V1 to V3, TEO to TEp, and TEp to AMY all registering periods of significant strengthening or weakening FC. The specific mechanisms that underlie FC changes in visual cortical areas in early infancy are still poorly understood and remain speculative. Nevertheless, region-specific patterns likely reflect local differences in the timing and progression of neuroanatomical and neurophysiological processes, in particular synaptic proliferation, reorganization, pruning, and myelination (Rakic et al., 1986; Webster et al., 1991a; Goodman and Shatz, 1993; Malkova et al., 2006; Elston et al., 2009, 2010; Kim et al., 2020).

By 2 weeks of age, the structure of visual cortex closely resembles that of the adult visual system – the quantity and distribution of cell types are similar (Kiorpes, 2015), as are the subcortical projections to V1 and the cortical projections from V1 (Baldwin et al., 2012). This existing structure may support the strong connectivity between the primary and extrastriate visual areas at birth (highest among all regions in the visual object pathway), and act as a scaffold for continued synaptogenesis and synaptic reorganization. The rate of synaptogenesis in visual cortex proceeds relative to conception, but the size, symmetry, and location of synaptic contacts are dependent on early visual experience (Bourgeois et al., 1989). By 4 months of age, cortical thickness (Bourgeois and Rakic, 1993) and synpatic density in visual cortex (Rakic et al., 1986; Elston et al., 2010) are at their peak, and most cells show adult-like functional properties – that is, they are responsive to visual stimuli and orientation selective (Rodman et al., 1993). This timing directly aligns with the period of greatest increase in FC between V1 and V3 presented in our results. After 4 months of age, synaptic density in visual areas begins to decrease, primarily due to the pruning of synapses on dendritic spines, which outpaces spinogenesis (Rakic et al., 1986; Elston et al., 2010). As this remarkable reorganization of visual cortex grey matter occurs from 0 to 6 months, white matter microstructure matures in parallel (Kim et al., 2020). Kim et al., 2020 showed that FA and MD in the occipital lobe, measures of white matter organization and integrity, develop at their greatest rate until about 9 months of age.

Unlike visual cortex, the structural and neurophysiological properties of inferior temporal cortex are less adult-like in early infancy. While TEO and TE also undergo rapid synaptogenesis and spine growth in early infancy – spine density doubles from 3 weeks to 3.5 months (Elston et al., 2010) – the rate of spinogenesis exceeds pruning and the receptive fields of neurons in TEO and TE continue to expand into adulthood (Elston et al., 2010). The signal response to visual stimuli, measured from 5 weeks to 7 months, is also less than in adulthood and the responses are more variable, suggesting signaling in inferior temporal cortex develops through the juvenile stage (Rodman et al., 1993; Rodman, 1994). Finally, the more posterior regions, closest to the visual extrastriate areas, have early increases in metabolic activity, whereas the anterior regions have a delayed increase (Webster et al., 1991a). Evidence from histological, electrophysiological, and metabolic studies in infant monkeys show that cortical areas along the visual object pathway mature progressively during the first 4 months after birth, from the most posterior occipital areas (V1-V3) towards the most anterior temporal areas (Rodman et al., 1991; Webster et al., 1991a; Distler et al., 1996), corroborating existing evidence that early brain maturation follows gradients of caudal to rostral maturation and the development of primary sensory regions before integrative cortices (Sydnor et al., 2021). All these factors may contribute to the less pronounced change measured in FC between V3 and TEO and TEO and TEp, relative to V1 and V3, and ultimately, the varied trajectories of FC along the regions of temporal cortex – i.e., TEO to TEp vs. TEp to AMY.

Mapping FC trajectories in the left and right hemispheres also revealed leftward lateralization in FC between V1 to V3. This finding is novel but aligns with structural results from other longitudinal studies in rhesus macaques which report leftward biases in brain-wide volume from 0 to 20 months (Scott et al., 2016; Kim et al., 2020) and more specifically, in cortical surface area, cortical thickness, and white matter volume in occipital cortex from 0 to 6 months (Kim et al., 2020; Xia et al., 2020). Xia et al., 2020 found leftward lateralization of cortical

surface area and thickness in occipital cortex increased from 0 to 7 months and then stabilized over time. In this study, leftward lateralization of FC in V1 to V3 was most prominent after 3 months.

Despite the region-specific differences measured in FC across the regions of the visual object pathway, the first 3 months of life consistently registered as the period of most significant and dynamic change in infant macaques. The neurophysiological properties of these regions, which are so responsive to early sensory experience, promote visual specialization and may contribute to the measured increase in the signal-to-noise ratio of the visual system that occurs during infancy (Goodman and Shatz, 1993; Bourne, 2010; Kiorpes, 2015). This pattern parallels brain development in human infants (Holland et al., 2014; Gao et al., 2015) and aligns directly with the period of most significant change in attention to the eyes.

4.2. Social attention to the eyes of conspecifics

The first 3 months of life also contained the period of greatest increase in attention to the eyes, followed by a period of increased individual variability from 4 to 6 months (Fig. 4B). These inflection points map closely to important social milestones in infant macaque development (Wang et al., 2020). Through the first 1.5 months of life, infant macaques are kept in close contact with their mothers and engage in increasingly frequent moments of mutual gaze and lip-smacking (Ferrari et al., 2009). After this period, infants gain the independence to explore and play at longer distances from their mothers. Play with other young infants takes center stage, and infant macaques begin to learn where they fall in the social hierarchy that defines their group structure.

The principal components (PCs) of variance extracted by FPCA align directly with these two stages (Fig. 4A). PC2 highlighted a period of increased variability around 1 to 3 months where infants have either an earlier or delayed increase and plateau in eye-looking. This period aligns with the stage when infants are in close physical contact with their mothers but are beginning to explore and play further away from them. In comparison, PC1 highlighted a second period of increased variability from 4 to 6 months during which infants increase or decrease their attention to eyes. Changing attention to the eyes in this period would be an adaptive skill as infants begin to immerse themselves in more frequent and complex social interactions with other members of their groups and begin to learn the use of gaze cues to communicate with others.

The group trajectory of eye-looking mapped here using FPCA is remarkably similar to that mapped by Wang et al. (2020) using polynomial models. When compared with results from Jones and Klin (2013), who used FPCA to map trajectories of eye-looking in human infants, we again emphasize the remarkable homology between eye-looking trajectories in human infants and infant macaques.

4.3. Accelerated trajectories of eye-looking are predicted by functional connectivity between the visual areas and social rank

For the first time, we identified features of brain development and social experience that influence eye-looking in infant rhesus macaques. Greater increases in early FC between left V1 and V3 predicted earlier increases in visual attention to the eyes of conspecifics in the first two months of life. We observed no associations between trajectories of attention to the mouth or body, suggesting activity between the left visual areas specifically supports attention to the eyes of conspecifics in the first weeks of life (Figs. S3 and S4).

In older macaques, the visual object pathway facilitates complex social cognition, in part due to a collection of neurons called the 'face patch' located in inferior temporal cortex, which has been compared to the human fusiform face area. At birth, neurons in inferior temporal cortex show adult-like firing patterns (Rodman et al., 1991) and have a clear foveal bias (Arcaro and Livingstone, 2017), but the 'patch' itself doesn't fully specialize for face recognition until 5 to 6 months of age (Livingstone et al., 2017). The maturation of the face patch is experience-dependent (Arcaro et al., 2017), so the association we find between V1 to V3 FC and eye-looking may serve as an early driver of neural specialization: V1 to V3 FC supports early eye-looking, visual experience that capitalizes on the architecture and physiology of the face patch system to promote processing of face information and social visual cues. The delayed maturation of the patch may also be why we did not observe associations between connectivity in the more anterior regions of the visual object pathway (TEp to AMY) and eye-looking. Future studies may need to extend imaging in a larger sample out to 9 or 12 months.

Attention to biological motion cues such as facial expressions and eye movements is also known to trigger activity in cortical areas within the motion pathway from V1 to medial temporal cortex (MT) to STS (Bremmer et al., 1997; Furl et al., 2012; Marciniak et al., 2014), as described by Pitcher and Ungerleider (2021). Although our study did not specifically analyze the development of FC within this pathway, an earlier report (Kovacs-Balint et al., 2019) indicated that FC change between V3–MT was moderate but stable from 0 to 3 months of age. They also found FC from MT to the anterior superior temporal area increased slightly from 0 to 3 months, suggesting continued maturation of FC in later infancy. Thus, we speculate that FC changes within cortical areas in STS may occur later as they do for face patch areas in inferior temporal cortex (around 5 to 6 months) (Arcaro and Livingstone, 2017). Additional studies of FC development in the motion pathway in relation to social visual engagement and social status are clearly warranted.

Further analysis showed the brain-behavior relationship between FC in left V1 to V3 and eye-looking was moderated by social rank, such that increases in left V1 to V3 connectivity predicted more accelerated increases in eye-looking for infants with lower social status and more delayed increases in eye-looking for infants with higher social status. In our small sample, we did not find an independent association between social rank and PC1 scores from V1 to V3 FC, indicating that LSS infants did not show faster V1 to V3 FC maturation than HSS infants. Rather we hypothesize that V1 to V3 FC maturation supports earlier eye-looking in LSS infants to potentially accelerate the development of pathways that allow LSS infants to identify and process eye-specific social cues from other macaques. This change may serve as a neurobehavioral adaptation for LSS infants to promote vigilance to the social environment and prepare subordinate infants to process salient socio-visual cues as early (and fast) as possible, allowing them to successfully monitor and navigate potentially aggressive social interactions.

This hypothesis is supported by growing evidence from both humans and macaques that exposure to early life social adversity accelerates neurobehavioral development (Belsky, 2019; Colich et al., 2020; Tooley et al., 2021). Early adversity is a broad construct, and different experiences of adversity - e.g., exposure to threat versus low socioeconomic status (SES) – appear to exert disparate impacts on brain maturation. For example, children who experience threat show greater cortical thinning in prefrontal networks, whereas children from low SES environments show greater thinning in visual and default mode networks (Colich et al., 2020). Additional biological markers of early maturation, like earlier emergence of molar teeth and onset of puberty, also occur in children from households who experienced physical or psychological stressors (McDermott et al., 2021). LSS macaques live in a continuously threatening social environment where they experience constant harassment and physical injuries. Findings from a cohort of juvenile rhesus macaques showed LSS females had higher FA than HSS females in white matter tracts connecting areas critical for decision making, the medial prefrontal cortex and corticothalamic fibers (Howell et al., 2014). Ultimately, the differential social environments conferred by low vs. high social status act as experiential forces with marked impacts on the development of social brain and, as we show here, behavior.

4.4. Advantages of nonparametric curve-fitting approaches

This study joins the body of literature showcasing the utility and advantage of using nonparametric modeling approaches, in particular FPCA, to map developmental change and test for associations between dynamic neurobehavioral processes (Jones and Klin, 2013; Dai et al., 2019b, 2019a; Chen et al., 2021). Here, we identify developmental milestones in trajectories of social visual attention and functional brain development in a data-driven manner. Moreover, we model summary scores of these milestones using multivariate statistics to identify relationships between those milestones. We believe this work highlights the promise of this method and motivates continued efforts with larger samples to investigate more robust associations between brain and behavior. Mapping typical development at high resolution in animal models of social development allows us to identify how deviations may arise in neurodevelopmental disability.

5. Limitations

MRI scans were completed after the administration of low levels of anesthesia. Decreased amounts of anesthesia relative to other rs-fMRI NHP studies were used to minimize the potential effects of isoflurane and telazol on functional activity and subsequent BOLD signal (Vincent et al., 2007; Hutchison et al., 2013; Li et al., 2013a), however FC differences with wakeful states may still exist (Jovellar and Doudet, 2019). Of note, these previous studies reported similar changes in BOLD signal between awake versus anesthetized macaques, particularly in signal from the visual system (Vincent et al., 2007; Hutchison et al., 2013; Li et al., 2013a). Moreover, one study specifically found levels of isoflurane below 1.5% of body weight led to no measured differences in cerebral blood flow in cortical regions (Li et al., 2013a). Differences were observed in the thalamus and cerebellum, critical subcortical regions, so the possible downstream effect of applied anesthesia cannot be dismissed. At the individual level, Kovacs-Balint et al. (2019) found controlling for levels of telazol and isoflurane in the same protocol and partial sample used in this study did not change the FC results in the visual object pathway.

The use of only male subjects in the sample was an additional limitation of this study. This decision was made to avoid the confounding effects of early sex differences in neurodevelopment and increase overall statistical power. The final sample of infant macaques also prioritized individuals from middle-ranking families. Though this criterion resulted in a reasonable range of values for the social status analysis, the final sample does not represent the complete range of possible statuses in macaque family groups. Finally, as mentioned in the Results section, our sample size was too small to detect statistically significant brain-behavior associations after correction for multiple comparisons. Future studies are necessary to replicate those results and to map trajectories of social neurobehavioral development across all members of the social hierarchy, and in female infants.

6. Citation diversity statement

Given recent work highlighting gendered citation biases in many scientific fields (Caplar et al., 2017;Teich et al., 2021), including neuroscience (Dworkin et al., 2020b), we include this citation diversity statement to reflect on sources of bias in our own citation practice (Dworkin et al., 2020a; Zurn et al., 2020). Predicted gender of the first and last author of each reference was determined through databases that measure the likelihood of a name being held by a man or woman or through personal knowledge of the authors. Of the references supporting this article, 30% were authored by man(first)/man(last), 19% by woman (first)/woman(last), 21% by woman(first)/man(last), and 15% by man (first)/woman(last). A man solo-authored 11% of references and a woman, 4% of references. These metrics exclude articles with the same first or senior author as this article and 1 paper where the first name of the first author could not be determined. While not an equitable distribution, our citation metrics reflect more gender diversity than the broader rates of authorship by gender in neuroscience over the last 25 years (Dworkin et al., 2020b). However, these measures are limited in that they primarily rely on a prediction of gender, rather than personal identification from each author. They also do not reflect other dimensions of identity that are known to influence citation bias, including race, ethnicity, and gender or queer identities beyond the man/woman binary.

Funding Sources

This work was supported by the National Institutes of Health (NIH, United States of America (USA)) grant numbers MH100029, MH078105–01S1, MH078105–04S1, MH119251, MH091645, MH086633, MH096773, K99/R00 MH091238, Eunice Kennedy Shriver National Institute of Child Health and Human Development (USA) U54 HD079124, National Institute of Biomedical Imaging and Bioengineering (USA) EB027147, National Library of Medicine (USA) T15LM007088, the Oregon Clinical and Translational Institute (USA, grant number CTSA UL1TR000128), the Masonic Institute for the Developing Brain, the Lynne and Andrew Redleaf Foundation, and the NIH's Office of the Director, Office of Research Infrastructure Programs, P51OD011132 (Emory National Primate Research Center (ENPRC) Base Grant). The ENPRC is fully accredited by AAALAC, International.

CRediT authorship contribution statement

Aiden Ford: Conceptualization, Formal analysis, Writing – original draft, Writing – review & editing, Visualization. **Zsofia Kovacs-Balint**: Conceptualization, Resources, Investigation, Data curation, Writing – review & editing, Supervision, Project administration. **Arick Wang**: Conceptualization, Writing – review & editing. **Eric Feczko**: Methodology, Software, Writing – review & editing. **Eric Earl**: Methodology, Software, Writing – review & editing. **Oscar Miranda-Dominguez**: Methodology, Software, Writing – review & editing. **Longchuan Li**: Methodology, Writing – review & editing. **Martin Styner**: Methodology, Software, Writing – review & editing. **Damien Fair**: Methodology, Software, Writing – review & editing. **Warren Jones**: Methodology, Software, Resources, Data curation, Writing – review & editing. **Jocelyne Bachevalier**: Conceptualization, Investigation, Resources, Writing – review & editing, Project administration, Funding acquisition. **Mar Sanchez**: Conceptualization, Investigation, Resources, Writing – review & editing, Supervision, Project administration, Funding acquisition.

Declaration of Competing Interest

The authors declare that they have no known competing financial interests or personal relationships that could have appeared to influence the work reported in this paper.

Data availability

Data will be made available on request.

Acknowledgments

Many thanks to Dr. Xiongtao Dai at University of California, Berkeley, for advice on functional data analysis, Dr. Lisa Parr, Trina Jonesteller, Shannon Moss, Jenna Brooks, Marie Collantes, Ruiyue Hong, and Madison Wallace at the Emory National Primate Research Center (ENPRC) Field Station, and Ruth Connelly, Sudeep Patel, and Doty Kempf at the ENPRC Imaging Center.

Data Statement

Data from this study may be made available upon request.

Appendix A. Supporting information

Supplementary data associated with this article can be found in the online version at doi:10.1016/j.dcn.2023.101213.

References

Andersson, J.L., Skare, S., Ashburner, J., 2003. How to correct susceptibility distortions in spin-echo echo-planar images: application to diffusion tensor imaging. Neuroimage 20, 870–888.

Arcaro, M.J., Livingstone, M.S., 2017. A hierarchical, retinotopic proto-organization of the primate visual system at birth. Elife 6.

Arcaro, M.J., Schade, P.F., Vincent, J.L., Ponce, C.R., Livingstone, M.S., 2017. Seeing faces is necessary for face-domain formation. Nat. Neurosci. 20, 1404–1412.

Baldwin, M.K., Kaskan, P.M., Zhang, B., Chino, Y.M., Kaas, J.H., 2012. Cortical and subcortical connections of V1 and V2 in early postnatal macaque monkeys. J. Comp. Neurol. 520, 544–569.

Baron-Cohen, S., Wheelwright, S., Jolliffe, T., 1997. Is There a "Language of the Eyes"? Evidence from Normal Adults, and Adults with Autism or Asperger Syndrome. Vis. Cogn. 4, 311–331.

Belsky, J., 2019. Early-life adversity accelerates child and adolescent development. Curr. Dir. Psychol. Sci. 28, 241–246.

Berman, C.M., 1980. Early agonistic experience and rank acquisition among free-ranging infant rhesus monkeys. Int. J. Primatol. 1, 150–173.

Bernstein, I.S., 1976. Dominance, aggression and reproduction in primate societies. J. Theor. Biol. 60, 459–472.

Bernstein, I.S., 1988. Kinship and behavior in nonhuman primates. Behav. Genet 18, 511–524.

Bernstein, I.S., Gordon, T.P., Rose, R.M., 1974. Aggression and social controls in rhesus monkey (Macaca mulatta) groups revealed in group formation studies. Folia Prima (Basel) 21, 81–107.

Bourgeois, J.P., Rakic, P., 1993. Changes of synaptic density in the primary visual cortex of the macaque monkey from fetal to adult stage. J. Neurosci. 13, 2801–2820.

Bourgeois, J.P., Jastreboff, P.J., Rakic, P., 1989. Synaptogenesis in visual cortex of normal and preterm monkeys: evidence for intrinsic regulation of synaptic overproduction. Proc. Natl. Acad. Sci. USA 86, 4297–4301.

Bourne, J.A., 2010. Unravelling the development of the visual cortex: implications for plasticity and repair. J. Anat. 217, 449–468.

Bremmer, F., Ilg, U.J., Thiele, A., Distler, C., Hoffmann, K.P., 1997. Eye position effects in monkey cortex. I. Visual and pursuit-related activity in extrastriate areas MT and MST. J. Neurophysiol. 77, 944–961.

Caplar, N., Tacchella, S., Birrer, S., 2017. Quantitative evaluation of gender bias in astronomical publications from citation counts. Nat. Astron. 1.

Chen, Y., Dubey, P., Muller, H.G., Bruchhage, M., Wang, J.L., Deoni, S., 2021. Modeling sparse longitudinal data in early neurodevelopment. Neuroimage 237, 118079.

Colich, N.L., Rosen, M.L., Williams, E.S., McLaughlin, K.A., 2020. Biological aging in childhood and adolescence following experiences of threat and deprivation: A systematic review and meta-analysis. Psychol. Bull. 146, 721–764.

Dai, X., Muller, H.G., Wang, J.L., Deoni, S.C.L., 2019a. Age-dynamic networks and functional correlation for early white matter myelination. Brain Struct. Funct. 224, 535–551.

Dai, X., Hadjipantelis, P., Wang, J.L., Deoni, S.C.L., Muller, H.G., 2019b. Longitudinal associations between white matter maturation and cognitive development across early childhood. Hum. Brain Mapp. 40, 4130–4145.

Deoni, S.C., Mercure, E., Blasi, A., Gasston, D., Thomson, A., Johnson, M., Williams, S.C., Murphy, D.G., 2011. Mapping infant brain myelination with magnetic resonance imaging. J. Neurosci. 31, 784–791.

Dettmer, A.M., Kaburu, S.S., Simpson, E.A., Paukner, A., Sclafani, V., Byers, K.L., Murphy, A.M., Miller, M., Marquez, N., Miller, G.M., Suomi, S.J., Ferrari, P.F., 2016. Neonatal face-to-face interactions promote later social behaviour in infant rhesus monkeys. Nat. Commun. 7, 11940.

Distler, C., Bachevalier, J., Kennedy, C., Mishkin, M., Ungerleider, L.G., 1996. Functional development of the corticocortical pathway for motion analysis in the macaque monkey: a 14C-2-deoxyglucose study. Cereb. Cortex 6, 184–195.

D'Souza, D., Cole, V., Farran, E.K., Brown, J.H., Humphreys, K., Howard, J., Rodic, M., Dekker, T.M., D'Souza, H., Karmiloff-Smith, A., 2015. Face processing in Williams syndrome is already atypical in infancy. Front Psychol. 6, 760.

Dworkin, J., Zurn, P., Bassett, D.S., 2020a. In)citing action to realize an equitable future. Neuron 106, 890–894.

Dworkin, J.D., Linn, K.A., Teich, E.G., Zurn, P., Shinohara, R.T., Bassett, D.S., 2020b. The extent and drivers of gender imbalance in neuroscience reference lists. Nat. Neurosci. 23, 918–926.

Elston, G.N., Oga, T., Fujita, I., 2009. Spinogenesis and pruning scales across functional hierarchies. J. Neurosci. 29, 3271–3275.

Elston, G.N., Oga, T., Okamoto, T., Fujita, I., 2010. Spinogenesis and pruning from early visual onset to adulthood: an intracellular injection study of layer III pyramidal cells in the ventral visual cortical pathway of the macaque monkey. Cereb. Cortex 20, 1398–1408.

Embree, M., Michopoulos, V., Votaw, J.R., Voll, R.J., Mun, J., Stehouwer, J.S., Goodman, M.M., Wilson, M.E., Sanchez, M.M., 2013. The relation of developmental changes in brain serotonin transporter (5HTT) and 5HT1A receptor binding to emotional behavior in female rhesus monkeys: effects of social status and 5HTT genotype. Neuroscience 228, 83–100.

Emery, N.J., 2000. The eyes have it: the neuroethology, function and evolution of social gaze. Neurosci. Biobehav Rev. 24, 581–604.

Fair, D.A., et al., 2012. Distinct neural signatures detected for ADHD subtypes after controlling for micro-movements in resting state functional connectivity MRI data. Front Syst. Neurosci. 6, 80.

Fair, D.A., Dosenbach, N.U., Church, J.A., Cohen, A.L., Brahmbhatt, S., Miezin, F.M., Barch, D.M., Raichle, M.E., Petersen, S.E., Schlaggar, B.L., 2007. Development of distinct control networks through segregation and integration. Proc. Natl. Acad. Sci. USA 104, 13507–13512.

Fair, D.A., Cohen, A.L., Power, J.D., Dosenbach, N.U., Church, J.A., Miezin, F.M., Schlaggar, B.L., Petersen, S.E., 2009. Functional brain networks develop from a "local to distributed" organization. PLoS Comput. Biol. 5, e1000381.

Farroni, T., Csibra, G., Simion, F., Johnson, M.H., 2002. Eye contact detection in humans from birth. Proc. Natl. Acad. Sci. USA 99, 9602–9605.

Ferrari, P.F., Paukner, A., Ionica, C., Suomi, S.J., 2009. Reciprocal face-to-face communication between rhesus macaque mothers and their newborn infants. Curr. Biol. 19, 1768–1772.

Furl, N., Hadj-Bouziane, F., Liu, N., Averbeck, B.B., Ungerleider, L.G., 2012. Dynamic and static facial expressions decoded from motion-sensitive areas in the macaque monkey. J. Neurosci. 32, 15952–15962.

Gao, W., Alcauter, S., Elton, A., Hernandez-Castillo, C.R., Smith, J.K., Ramirez, J., Lin, W., 2015. Functional network development during the first year: relative sequence and socioeconomic correlations. Cereb. Cortex 25, 2919–2928.

Ghazanfar, A.A., Santos, L.R., 2004. Primate brains in the wild: the sensory bases for social interactions. Nat. Rev. Neurosci. 5, 603–616.

Gilmore, J.H., Knickmeyer, R.C., Gao, W., 2018. Imaging structural and functional brain development in early childhood. Nat. Rev. Neurosci. 19, 123–137.

Godfrey, J.R., Pincus, M., Sanchez, M.M., 2016. Effects of social subordination on macaque neurobehavioral outcomes: focus on neurodevelopment. In: Shively, C.A., Wilson, M.E. (Eds.), Social Inequalities in Health in Nonhuman primates: The Biology of the Gradient. Springer International Publishing, Cambridge, pp. 25–47.

Goodman, C.S., Shatz, C.J., 1993. Developmental mechanisms that generate precise patterns of neuronal connectivity. Cell 72 (Suppl), 77–98.

Goren, C.C., Sarty, M., Wu, P.Y., 1975. Visual following and pattern discrimination of face-like stimuli by newborn infants. Pediatrics 56, 544–549.

Gorgolewski, K., Burns, C.D., Madison, C., Clark, D., Halchenko, Y.O., Waskom, M.L., Ghosh, S.S., 2011. Nipype: a flexible, lightweight and extensible neuroimaging data processing framework in python. Front Neuroinform 5, 13.

Holland, D., Chang, L., Ernst, T.M., Curran, M., Buchthal, S.D., Alicata, D., Skranes, J., Johansen, H., Hernandez, A., Yamakawa, R., Kuperman, J.M., Dale, A.M., 2014. Structural growth trajectories and rates of change in the first 3 months of infant brain development. JAMA Neurol. 71, 1266–1274.

Howell, B.R., Godfrey, J., Gutman, D.A., Michopoulos, V., Zhang, X., Nair, G., Hu, X., Wilson, M.E., Sanchez, M.M., 2014. Social subordination stress and serotonin transporter polymorphisms: associations with brain white matter tract integrity and behavior in juvenile female macaques. Cereb. Cortex 24, 3334–3349.

Hutchison, R.M., Womelsdorf, T., Gati, J.S., Everling, S., Menon, R.S., 2013. Resting-state networks show dynamic functional connectivity in awake humans and anesthetized macaques. Hum. Brain Mapp. 34, 2154–2177.

Johnson, M.H., Dziurawiec, S., Ellis, H., Morton, J., 1991. Newborns' preferential tracking of face-like stimuli and its subsequent decline. Cognition 40, 1–19.

Jones, W., Klin, A., 2013. Attention to eyes is present but in decline in 2-6-month-old infants later diagnosed with autism. Nature 504, 427–431.

Jovellar, D.B., Doudet, D.J., 2019. fMRI in Non-human Primate: A Review on Factors That Can Affect Interpretation and Dynamic Causal Modeling Application. Front Neurosci. 13, 973.

Kim, J., Jung, Y., Barcus, R., Bachevalier, J.H., Sanchez, M.M., Nader, M.A., Whitlow, C. T., 2020. Rhesus Macaque Brain Developmental Trajectory: A Longitudinal Analysis Using Tensor-Based Structural Morphometry and Diffusion Tensor Imaging. Cereb. Cortex 30, 4325–4335.

Kiorpes, L., 2015. Visual development in primates: Neural mechanisms and critical periods. Dev. Neurobiol. 75, 1080–1090.

Kosakowski, H.L., Cohen, M.A., Takahashi, A., Keil, B., Kanwisher, N., Saxe, R., 2021. Selective responses to faces, scenes, and bodies in the ventral visual pathway of infants. Curr. Biol.

Kovacs-Balint, Z., Feczko, E., Pincus, M., Earl, E., Miranda-Dominguez, O., Howell, B., Morin, E., Maltbie, E., Li, L., Steele, J., Styner, M., Bachevalier, J., Fair, D., Sanchez, M., 2019. Early Developmental Trajectories of Functional Connectivity Along the Visual Pathways in Rhesus Monkeys. Cereb. Cortex 29, 3514–3526.

Kovacs-Balint, Z.A., Payne, C., Steele, J., Li, L., Styner, M., Bachevalier, J., Sanchez, M. M., 2021. Structural development of cortical lobes during the first 6 months of life in infant macaques. Dev. Cogn. Neurosci. 48, 100906.

Ku, S.P., Tolias, A.S., Logothetis, N.K., Goense, J., 2011. fMRI of the face-processing network in the ventral temporal lobe of awake and anesthetized macaques. Neuron 70, 352–362.

Kuwahata, H., Adachi, I., Fujita, K., Tomonaga, M., Matsuzawa, T., 2004. Development of schematic face preference in macaque monkeys. Behav. Process. 66, 17–21.

Lewis, J.W., Van Essen, D.C., 2000. Corticocortical connections of visual, sensorimotor, and multimodal processing areas in the parietal lobe of the macaque monkey. J. Comp. Neurol. 428, 112–137.

Li, C.X., Patel, S., Auerbach, E.J., Zhang, X., 2013a. Dose-dependent effect of isoflurane on regional cerebral blood flow in anesthetized macaque monkeys. Neurosci. Lett. 541, 58–62.
Li, G., Nie, J., Wang, L., Shi, F., Lin, W., Gilmore, J.H., Shen, D., 2013b. Mapping region-specific longitudinal cortical surface expansion from birth to 2 years of age. Cereb. Cortex 23, 2724–2733.
Livingstone, M.S., Vincent, J.L., Arcaro, M.J., Srihasam, K., Schade, P.F., Savage, T., 2017. Development of the macaque face-patch system. Nat. Commun. 8, 14897.
Machado, C.J., Bachevalier, J., 2003. Non-human primate models of childhood psychopathology: the promise and the limitations. J. Child Psychol. Psychiatry 44, 64–87.
Malkova, L., Heuer, E., Saunders, R.C., 2006. Longitudinal magnetic resonance imaging study of rhesus monkey brain development. Eur. J. Neurosci. 24, 3204–3212.
Mandalaywala, T.M., Parker, K.J., Maestripieri, D., 2014. Early experience affects the strength of vigilance for threat in rhesus monkey infants. Psychol. Sci. 25, 1893–1902.
Marciniak, K., Atabaki, A., Dicke, P.W., Thier, P., 2014. Disparate substrates for head gaze following and face perception in the monkey superior temporal sulcus. Elife 3.
Markov, N.T., et al., 2014. A weighted and directed interareal connectivity matrix for macaque cerebral cortex. Cereb. Cortex 24, 17–36.
Mattison, J.A., Vaughan, K.L., 2017. An overview of nonhuman primates in aging research. Exp. Gerontol. 94, 41–45.
May, T., Adesina, I., McGillivray, J., Rinehart, N.J., 2019. Sex differences in neurodevelopmental disorders. Curr. Opin. Neurol. 32, 622–626.
McDermott, C.L., Hilton, K., Park, A.T., Tooley, U.A., Boroshok, A.L., Mupparapu, M., Scott, J.M., Bumann, E.E., Mackey, A.P., 2021. Early life stress is associated with earlier emergence of permanent molars. Proc. Natl. Acad. Sci. USA 118.
Miranda-Dominguez, O., Mills, B.D., Grayson, D., Woodall, A., Grant, K.A., Kroenke, C. D., Fair, D.A., 2014. Bridging the gap between the human and macaque connectome: a quantitative comparison of global interspecies structure-function relationships and network topology. J. Neurosci. 34, 5552–5563.
Morrill, R.J., Paukner, A., Ferrari, P.F., Ghazanfar, A.A., 2012. Monkey lipsmacking develops like the human speech rhythm. Dev. Sci. 15, 557–568.
Mosher, C.P., Zimmerman, P.E., Gothard, K.M., 2011. Videos of conspecifics elicit interactive looking patterns and facial expressions in monkeys. Behav. Neurosci. 125, 639–652.
Muschinski, J., Feczko, E., Brooks, J.M., Collantes, M., Heitz, T.R., Parr, L.A., 2016. The development of visual preferences for direct versus averted gaze faces in infant macaques (Macaca mulatta). Dev. Psychobiol. 58, 926–936.
Parr, L.A., 2011. The evolution of face processing in primates. Philos. Trans. R. Soc. Lond. B Biol. Sci. 366, 1764–1777.
Parr, L.A., Murphy, L., Feczko, E., Brooks, J., Collantes, M., Heitz, T.R., 2016. Experience-dependent changes in the development of face preferences in infant rhesus monkeys. Dev. Psychobiol. 58, 1002–1018.
Passingham, R., 2009. How good is the macaque monkey model of the human brain? Curr. Opin. Neurobiol. 19, 6–11.
Paukner, A., Slonecker, E.M., Murphy, A.M., Wooddell, L.J., Dettmer, A.M., 2018. Sex and rank affect how infant rhesus macaques look at faces. Dev. Psychobiol. 60, 187–193.
Pincus, M., Godfrey, J.R., Feczko, E., Earl, E., Miranda-Dominguez, O., Fair, D., Wilson, M.E., Sanchez, M.M., Kelly, C., 2021. Chronic psychosocial stress and experimental pubertal delay affect socioemotional behavior and amygdala functional connectivity in adolescent female rhesus macaques. Psychoneuroendocrinology 127, 105154.
Pitcher, D., Ungerleider, L.G., 2020. Evidence for a third visual pathway specialized for social perception. Trends Cogn. Sci.
Powell, L.J., Kosakowski, H.L., Saxe, R., 2018. Social origins of cortical face areas. Trends Cogn. Sci. 22, 752–763.
Rakic, P., Bourgeois, J.P., Eckenhoff, M.F., Zecevic, N., Goldman-Rakic, P.S., 1986. Concurrent overproduction of synapses in diverse regions of the primate cerebral cortex. Science 232, 232–235.
Rilling, J.K., 2014. Comparative primate neuroimaging: insights into human brain evolution. Trends Cogn. Sci. 18, 46–55.
Rodman, H.R., 1994. Development of inferior temporal cortex in the monkey. Cereb. Cortex 4, 484–498.
Rodman, H.R., Skelly, J.P., Gross, C.G., 1991. Stimulus selectivity and state dependence of activity in inferior temporal cortex of infant monkeys. Proc. Natl. Acad. Sci. USA 88, 7572–7575.
Rodman, H.R., Scalaidhe, S.P., Gross, C.G., 1993. Response properties of neurons in temporal cortical visual areas of infant monkeys. J. Neurophysiol. 70, 1115–1136.
Roy, A., Shepherd, S.V., Platt, M.L., 2014. Reversible inactivation of pSTS suppresses social gaze following in the macaque (Macaca mulatta). Soc. Cogn. Affect Neurosci. 9, 209–217.
Santos, S., Ferreira, H., Martins, J., Goncalves, J., Castelo-Branco, M., 2022. Male sex bias in early and late onset neurodevelopmental disorders: Shared aspects and differences in Autism Spectrum Disorder, Attention Deficit/hyperactivity Disorder, and Schizophrenia. Neurosci. Biobehav Rev. 135, 104577.
Scott, J.A., Grayson, D., Fletcher, E., Lee, A., Bauman, M.D., Schumann, C.M., Buonocore, M.H., Amaral, D.G., 2016. Longitudinal analysis of the developing rhesus monkey brain using magnetic resonance imaging: birth to adulthood. Brain Struct. Funct. 221, 2847–2871.
Shi, Y., Budin, F., Yapuncich, E., Rumple, A., Young, J.T., Payne, C., Zhang, X., Hu, X., Godfrey, J., Howell, B., Sanchez, M.M., Styner, M.A., 2016. UNC-Emory Infant Atlases for Macaque Brain Image Analysis: Postnatal Brain Development through 12 Months. Front Neurosci. 10, 617.
Shultz, S., Klin, A., Jones, W., 2018. Neonatal transitions in social behavior and their implications for autism. Trends Cogn. Sci. 22, 452–469.
Smith, S.M., Jenkinson, M., Woolrich, M.W., Beckmann, C.F., Behrens, T.E., Johansen-Berg, H., Bannister, P.R., De Luca, M., Drobnjak, I., Flitney, D.E., Niazy, R.K., Saunders, J., Vickers, J., Zhang, Y., De Stefano, N., Brady, J.M., Matthews, P.M., 2004. Advances in functional and structural MR image analysis and implementation as FSL. Neuroimage 23 (Suppl 1), S208–S219.
Snyder-Mackler, N., Kohn, J.N., Barreiro, L.B., Johnson, Z.P., Wilson, M.E., Tung, J., 2016. Social status drives social relationships in groups of unrelated female rhesus macaques. Anim. Behav. 111, 307–317.
Styner, M., Knickmeyer, R., Joshi, S., Coe, C., Short, S.J., Gilmore, J., 2007. Automatic brain segmentation in rhesus monkeys. Med. Imaging 2007: Image Process.
Suomi, S.J., 2005. Mother-infant attachment, peer relationships, and the development of social networks in rhesus monkeys. Hum. Dev. 48, 67–79.
Sydnor, V.J., Larsen, B., Bassett, D.S., Alexander-Bloch, A., Fair, D.A., Liston, C., Mackey, A.P., Milham, M.P., Pines, A., Roalf, D.R., Seidlitz, J., Xu, T., Raznahan, A., Satterthwaite, T.D., 2021. Neurodevelopment of the association cortices: Patterns, mechanisms, and implications for psychopathology. Neuron 109, 2820–2846.
Erin G. Teich, Jason Z. Kim, Christopher W. Lynn, Samantha C. Simon, Andrei A. Klishin, Karol P. Szymula, Pragya Srivastava, Lee C. Bassett, Perry Zurn, Dworkin J.D., Bassett D.S. (2021) Citation inequity and gendered citation practices in contemporary physics. arXiv:1–16.
Tooley, U.A., Bassett, D.S., Mackey, A.P., 2021. Environmental influences on the pace of brain development. Nat. Rev. Neurosci. 22, 372–384.
Ungerleider, L.G., Bell, A.H., 2011. Uncovering the visual "alphabet": advances in our understanding of object perception. Vis. Res 51, 782–799.
Valenza, E., Simion, F., Cassia, V.M., Umilta, C., 1996. Face preference at birth. J. Exp. Psychol. Hum. Percept. Perform. 22, 892–903.
Vincent, J.L., Patel, G.H., Fox, M.D., Snyder, A.Z., Baker, J.T., Van Essen, D.C., Zempel, J. M., Snyder, L.H., Corbetta, M., Raichle, M.E., 2007. Intrinsic functional architecture in the anaesthetized monkey brain. Nature 447, 83–86.
de Waal, F.B.M., Luttrell, L.M., 1985. The formal hierarchy of rhesus macaques: An investigation of the bared-teeth display. Am. J. Prima 9, 73–85.
Wang, A., Payne, C., Moss, S., Jones, W.R., Bachevalier, J., 2020. Early developmental changes in visual social engagement in infant rhesus monkeys. Dev. Cogn. Neurosci. 43, 100778.
Wang, J.-L., Chiou, J.-M., Müller, H.-G., 2015. Review of functional data analysis. Annu Rev. Stat. 2015, 1–41.
Webster, M.J., Ungerleider, L.G., Bachevalier, J., 1991a. Connections of inferior temporal areas TE and TEO with medial temporal-lobe structures in infant and adult monkeys. J. Neurosci. 11, 1095–1116.
Webster, M.J., Ungerleider, L.G., Bachevalier, J., 1991b. Lesions of inferior temporal area TE in infant monkeys alter cortico-amygdalar projections. Neuroreport 2, 769–772.
White, L.E., Hinde, R.A., 1975. Some factors affecting mother-infant relations in rhesus monkeys. Anim. Behav. 23, 527–542.
Wilson, M.E., 2016. An Introduction to the Female Macaque Model of Social Subordination Stress. In: Shively, C.A., Wilson, M.E. (Eds.), Social Inequalities in Health in Nonhuman primates: The Biology of the Gradient. Springer International Publishing, Cambridge, pp. 9–24.
Wooddell, L.J., Kaburu, S.S.K., Dettmer, A.M., 2020. Dominance rank predicts social network position across developmental stages in rhesus monkeys. Am. J. Prima 82, e23024.
Woolrich, M.W., Jbabdi, S., Patenaude, B., Chappell, M., Makni, S., Behrens, T., Beckmann, C., Jenkinson, M., Smith, S.M., 2009. Bayesian analysis of neuroimaging data in FSL. Neuroimage 45, S173–S186.
Xia, J., Wang, F., Wu, Z., Wang, L., Zhang, C., Shen, D., Li, G., 2020. Mapping hemispheric asymmetries of the macaque cerebral cortex during early brain development. Hum. Brain Mapp. 41, 95–106.
Yao, F., Müller, H.-G., Wang, J.-L., 2005. Functional data analysis for sparse longitudinal data. J. Am. Stat. Assoc. 100, 577–590.
Zurn, P., Bassett, D.S., Rust, N.C., 2020. The citation diversity statement: a practice of transparency, a way of life. Trends Cogn. Sci. 24, 669–672.